Fault Classification and Section Identification of an Advanced Series-Compensated Transmission Line Using Support Vector Machine

P. K. Dash, *Senior Member, IEEE*, S. R. Samantaray, and Ganapati Panda, *Senior Member, IEEE*

***Abstract*—Distance protection of flexible ac transmission lines, including the thyristor-controlled series compensator (TCSC), static synchronous compensator, and static var compensator has been a very challenging task. This paper presents a new approach for the protection of TCSC line using a support vector machine (SVM). The proposed method uses postfault current samples for half cycle (ten samples) from the inception of the fault and firing angle as inputs to the SVM. Three SVMs are trained to provide fault classification, ground detection, and section identification, respectively, for the line using TCSC. The SVMs are trained with polynomial kernel and Gaussian kernel with different parameter values to get the most optimized classifier. The proposed method converges very fast with fewer numbers of training samples compared to neural-network and neuro-fuzzy systems which indicates fastness and accuracy of the proposed method for protection of the transmission line with TCSC.**

***Index Terms*—Distance protection, flexible ac transmission system (FACTS) support vector machine (SVM), thyristor-controlled series compensator (TCSC).**

I. Introduction

THE USE of flexible ac transmission system (FACTS) devices to improve the power transfer capability in a high-voltage transmission line is of greater interest these days. The thyristor-controlled series compensator (TCSC) [1] is one of the main FACTS devices, which has the ability to improve the utilization of the existing transmission system. The TCSC-based compensation possesses a thyristor-controlled variable capacitor protected by a metal–oxide varistor (MOV) and an air gap. However, the implementation of this technology changes the apparent line impedance, which is controlled by the firing angle of thyristors, and is accentuated by other factors including the MOV. The presence of the TCSC in the fault loop not only affects the steady-state components but also the transient components. The controllable reactance, the MOVs protecting the capacitors, and the air gaps' operation make the protection decision more complex and, therefore, the conventional relaying scheme based on fixed settings has its limitations.

Manuscript received July 12, 2005. Paper no. TPWRD-00398-2005.

P. K. Dash is with the Center for Research in Electrical, Electronics and Computer Engineering, Bhubaneswar 751023, India (e-mail: pkdash_india@yahoo.com).

S. R. Samantaray and G. Panda are with the Department of Electronics and Communications Engineering, National Institute of Technology, Rourkela 769008, India (e-mail: sbh_samant@rediffmail.com; gpanda@nitrkl.ac.in).

Digital Object Identifier 10.1109/TPWRD.2006.876695

Fault classification and section identification is a very challenging task for a transmission line with TCSC. Different attempts have been made for fault classification using wavelet transform, the Kalman filtering approach, and neural network [4], [5].

The Kalman filtering approach finds its limitation, as fault resistance cannot be modeled and further it requires a number of different filters to accomplish the task. The back propagation neural network (BPNN), radial basis function neural network (RBFNN), and fuzzy neural network (FNN) are employed for the adaptive protection of such a line where the protection philosophy is viewed as a pattern classification problem [4], [5]. The networks generate the trip or block signals using a data window of voltages and currents at the relaying point. However, the above approaches are sensitive to system frequency changes, requiring large training sets, training time, and a large number of neurons.

This paper presents a new approach for fault classification and section identification of the TCSC-based line using a support vector machine (SVM). SVM is basically a classifier based on an optimization technique. It optimizes the classification boundary between two classes very close to each other and thereby classifies the data sets even very close to each other. Also, SVM works successfully for multiclass classification with SVM regression.

The current signals for all phases are retrieved at the relaying end at a sampling frequency of 1.0 kHz. Half-cycle data (ten samples) and firing angle are used as an input to the SVM. The SVM is trained with input and output sets to provide the most optimized boundary for classification. Also, another SVM is trained for identifying the TCSC position on the transmission line. Taking the current data samples before and after the TCSC, the corresponding SVM is trained to identify whether the fault includes TCSC or not. When the fault includes TCSC, the third and fifth harmonic components are highly pronounced compared to the fault which does not include the TCSC. This issue is taken care of by SVMs as the total half cycles (ten samples) data of the current signal are taken into consideration for training and testing the SVMs.

II. System Studied

A 400-kV, 50-Hz power system is illustrated in Fig. 1. In this system, a TCSC is located at the midpoint of the transmission line, used for the distance protection study. The power system consists of two sources, TCSC and associated components, and a 300-km transmission line. The transmission line

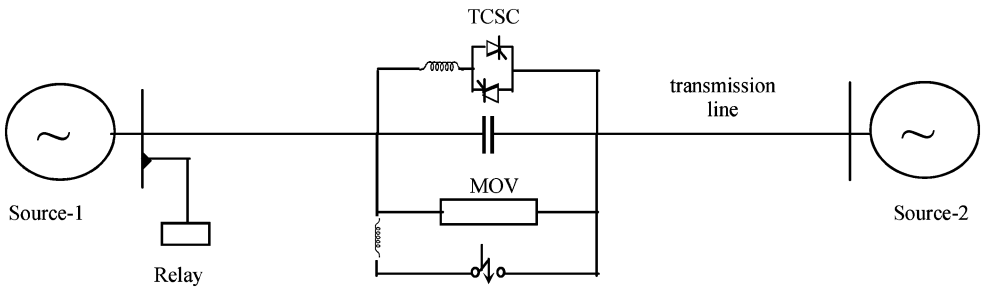

Fig. 1. TCSC-based line.

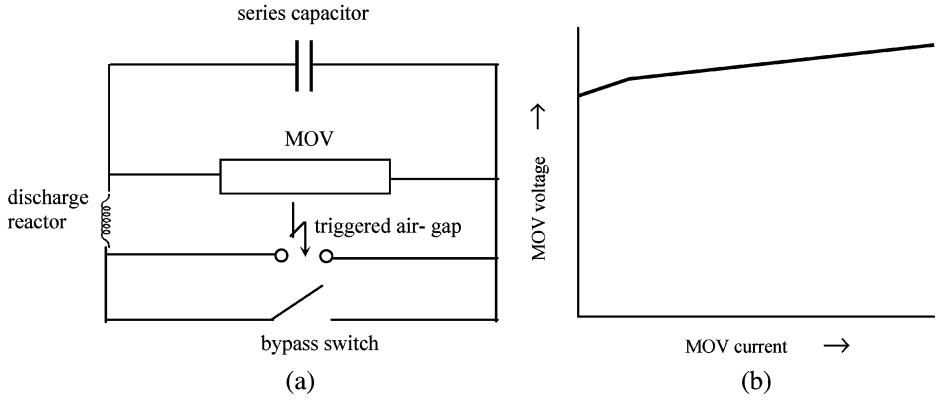

Fig. 2. (a) MOV protected series capacitor. (b) MOV characteristic.

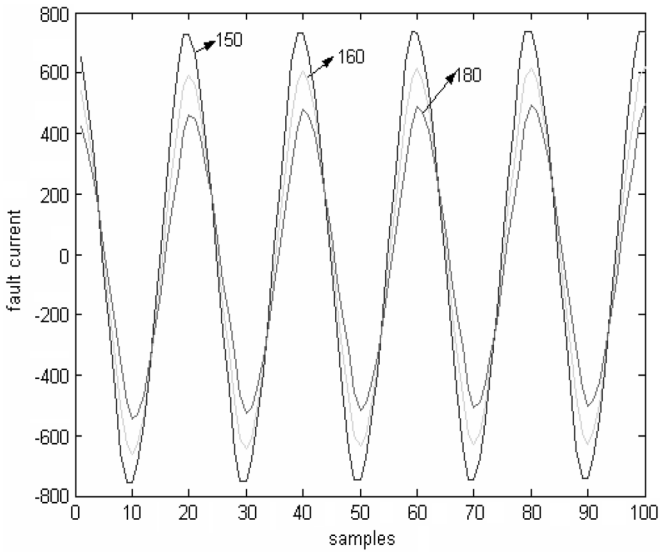

Fig. 3. Fault current with TCSC at different firing angles.

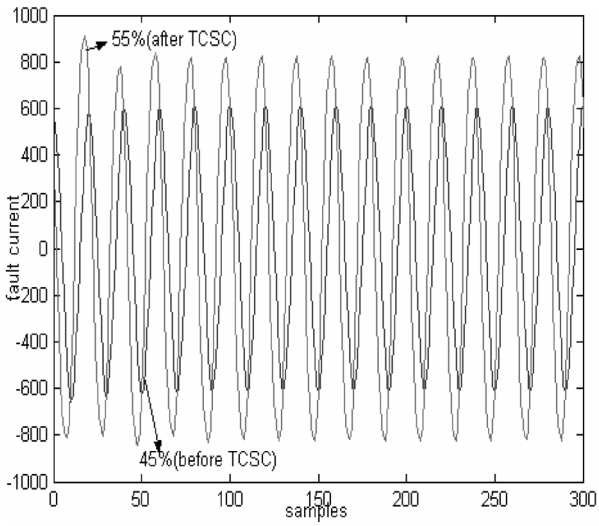

Fig. 4. Fault current before and after TCSC at the 160° firing angle.

has zero-sequence impedance $Z(0) = 96.45 + j335.26\ \mathrm{ohm}$ and positive-sequence impedance $Z(1) = 9.78 + j110.23\,\mathrm{ohm}$. $E_S = 400$ kV and $E_R = 400\angle\delta$ kV. The TCSC is designed to provide compensation varying from a minimum of 30% to a maximum of 40%. All of the components are modeled using the EMTDC subroutines. Fig. 3 shows the fault current at different firing angles and Fig. 4 shows the fault current before and after TCSC on the transmission line.

The sampling frequency is 1.0 kHz at the 50-Hz base frequency. The MOV consists of a number of zinc–oxide disks electrically connected in series and parallel. The purpose of the MOV is to prevent the voltage across the capacitor from rising to levels which will damage the capacitor. This is most likely to happen when a fault occurs at a point on the compensated line which minimizes the impedance of the fault loop. When instantaneous voltage across the capacitor approaches a dangerous level, the MOV begins to draw a significant proportion of the line current thereby limiting the voltage across the capacitor at that level. This action alters the impedance in the series path and, hence, the fault-loop impedance. In the event that the MOV remains in conduction long enough to raise its temperature (energy) to a dangerous level, an air gap is triggered to short out

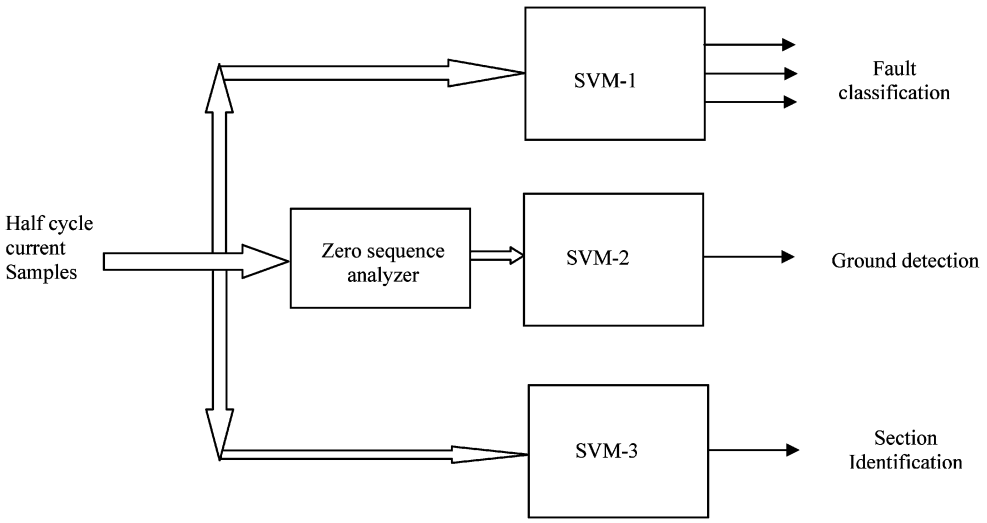

Fig. 6. Proposed scheme for protection. Fault classification (SVM-1), ground detection (SVM-2), and section identification (SVM-3).

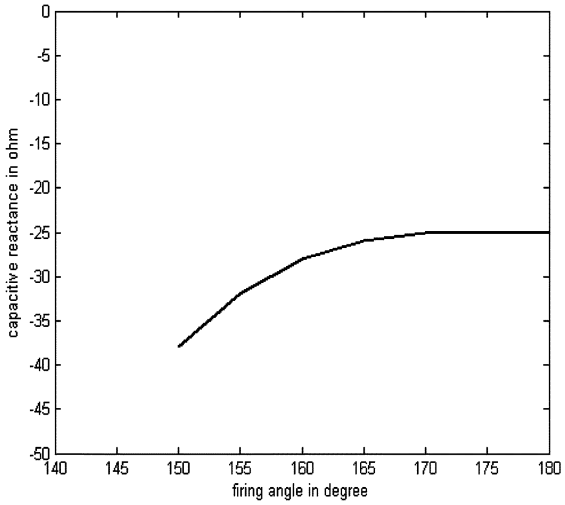

Fig. 5. Variation of capacitive reactance with the firing angle.

both the MOV and the capacitor, again changing the fault loop impedance. The operation of the MOV can be within the first half cycle of fault and depending on the severity of the fault, it may continue to operate until the air gap is triggered cycles later. This is precisely the time when a digital relay makes a protection decision. Further, a bypass switch in parallel with the gap automatically closes for abnormal system conditions that cause prolonged current flow through the gap. Fig. 2(a) shows a typical series capacitor arrangement for one phase of a transmission line and the typical voltage-current characteristic of an MOV is shown in Fig. 2(b).

The small inductance in the arrangement limits the current through the air gap or switch circuit. The TCSC is designed such that it provides 30% compensation at 180° (minimum) and 40% compensation at 150° (maximum) firing angle and, in this study, the firing angle is varied within this range as shown in Fig. 5. The proposed protection scheme is shown in Fig. 6.

The TCSC is placed at 50% of the transmission line with 300-km line length, which is 150 km from the relaying end. The simulation for all 11 types of shunt faults (L-G, LL-G, LL, LLL, LLL-G) is made on the transmission line with different fault resistance, source impedance, and incident angles at different fault locations with varying the firing angle from 150°–180° with (after) and without including (before) TCSC. The half-cycle signal having ten samples from the fault inception is retrieved at the relaying end and is normalized to be used as an input to the corresponding SVMs.

III. SVM for Classification

SVM [8]–[16] is a relatively new computational learning method based on the statistical learning theory. In SVM, the original input space is mapped into a high-dimensional dot product space called a feature space, and in the feature space, the optimal hyperplane is determined to maximize the generalization ability of the classifier. The optimal hyperplane is found by exploiting the optimization theory, and respecting insights provided by the statistical learning theory.

SVMs have the potential to handle very large feature spaces, because the training of SVM is carried out so that the dimension of classified vectors does not have as a distinct influence on the performance of SVM as it has on the performance of conventional classifiers. That is why it is noticed to be especially efficient in large classification problems. This will also benefit in fault classification, because the number of features to be the basis of fault diagnosis may not have to be limited. Also, SVM-based classifiers are claimed to have good generalization properties compared to conventional classifiers, because in training the SVM classifier, the so-called structural misclassification risk is to be minimized, whereas traditional classifiers are usually trained so that the empirical risk is minimized. SVM is compared to the radial basis function (RBF) neural network in an industrial fault classification task, and it has been found to give better generalization. SVMs may have problems with large data sets, but in the development of fault classification routines, these are usually not even available.

Let n-dimensional input $x_i (i = \ldots M)$, M be the number of samples) belong to class-I or Class-II, and associated labels be $y_i = 1$ for Class I and $y_i = -1$ for Class II, respectively. For

linearly separable data, we can determine a hyperplane $f(x) = 0$ that separates the data

$$f(x) = w^T x + b = \sum_{j=1}^{n} w_j x_j + b = 0 \tag{1}$$

where "w" is an n-dimensional vector and "b" is a scalar. The vector "w" and the scalar "b" determine the position of the separating hyperplane. Function $\mathrm{sign}(f(x))$ is also called the decision function. A distinctly separating hyperplane satisfies the constraints $f(x_\mathrm{i}) \geq 1$ if $y_i = +1$ and $f(x_i) \geq -1$, if $y_i = -1$. This results in

$$y_i f(x_i) = y_i(w^T x_i + b) \geq 1, \quad \text{for } i = 1, \ldots, \mathrm{M}. \tag{2}$$

The separating hyperplane that creates the maximum distance between the plane and the nearest data (i.e., the maximum margin) is called the optimal separating hyperplane. An example of the optimal separating hyperplane of two datasets is presented in Fig. 7. From the geometry, the geometrical margin is found to be $\|w\|^{-2}$. Taking into account the noise with slack variables ξ_i and error penalty C, the optimal hyperplane can be found by solving the following convex quadratic optimization problem:

minimize

$$\frac{1}{2}\|w\|^2 + C\sum_{i=1}^{M} \xi_i$$

subject to

$$y_i(w^T x_i + b) \geq 1 - \xi_\mathrm{i}, \quad \text{for } i = 1, \ldots, M$$
$$\xi_i \geq 0, \quad \text{for all } i \tag{3}$$

where ξ_i is measuring the distance between the margin and the examples x_i lying on the wrong side of the margin. The calculations can be simplified by converting the problem with Kuhn–Tucker conditions into the equivalent Lagrange dual problem, which will be

maximize

$$W(\alpha) = \sum_{i=1}^{M} \alpha_i - \frac{1}{2}\sum_{i,k=0}^{M} \alpha_i \alpha_k y_i y_k x_i^T x_k$$

subject to

$$\sum_{i=1}^{M} y_i \alpha_i = 0,\ C \geq \alpha_i \geq 0,\ i = 1, \ldots, M. \tag{4}$$

The number of variables of the dual problem is the number of training data. Let us denote the optimal solution of the dual problem with α^* and w^*. According to the Karush–Kuhn–Tucker theorem, the equality condition in (2) holds for the training input–output pair (xi, yi) only if the associated α^* is not 0. In this case, the training example x_i is a support vector (SV). Usually, the number of SVs is considerably lower than the number of training samples making SVM computationally very efficient. The value of the optimal bias b^* is found from the geometry

$$b^* = -\frac{1}{2}\sum_{\mathrm{SVs}} y_i \alpha_i^* \left(s_1^T x_i + s_2^T x_i\right) \tag{5}$$

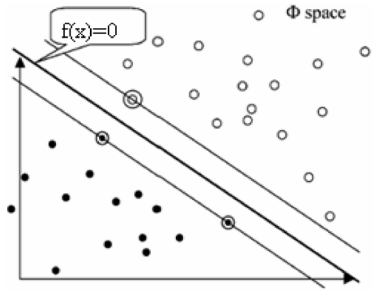

Fig. 7. $f(x)$ as a separating hyperplane lying in a high-dimensional space. Support vectors are inside the circles.

where s_1 and s_2 are arbitrary support vectors (SVs) for Class I and Class II, respectively. Only the samples associated with the SVs are summed, because the other elements of the optimal Lagrange multiplier α^* are equal to zero.

The final decision function will be given by

$$f(x) = \sum_{\mathrm{SVs}} \alpha_i y_i x_i^T x + b^*. \tag{6}$$

Then unknown data example "x" is classified as follows:

$$x \in \begin{cases} \mathrm{Class-I}, & \text{if } f(x) \geq 0 \\ \mathrm{Class-II}, & \text{otherwise.} \end{cases} \tag{7}$$

SVM can also be used in nonlinear classification tasks with the application of kernel functions. The data to be classified are mapped onto a high-dimensional feature space, where the linear classification is possible. Using a nonlinear vector function $\phi(x) = (\phi_1(x), \ldots, \phi_\mathrm{m}(x))$, $m \gg n$ to map the "n"-dimensional input vector "x" into the "m" dimensional feature space, the linear decision function in dual form is given by

$$\mathrm{f(x)} = \sum_{\mathrm{SVs}} \alpha_i y_i \phi^T(x_i)\phi(x). \tag{8}$$

Working in the high-dimensional feature space enables the expression of complex functions, but it also generates problems. Computational problems occur due to the large vectors and the danger of overfitting also exists due to the high dimensionality. The latter problem is solved above with the application of the maximal margin classifier, and so-called kernels give solution to the first problem. Notice that in (8) as well as in the optimization problem (3), the data occur only in inner products. A function that returns a dot product of the feature space mappings of original data points is called a kernel $K(x, z) = \phi^T(x)\phi(z)$. Applying a kernel function, the learning in the feature space does not require an explicit evaluation of ϕ. Using a kernel function, the decision function will be

$$f(x) = \sum_{\mathrm{SVs}} \alpha_i^* y_i K(x_i, x) \tag{9}$$

and the unknown data example is classified as before. The values of $K(x_i, x_j)$ over all training samples, $i, j = 1, \ldots, M$, form the kernel matrix, which is a central structure in the

TABLE I
TESTING OF SVM-1 FOR FAULT CLASSIFICATION

Fault	Kernel	Parameter value	a	b	c
b-g fault at 30%,α=155°,R_f =20 ohm	poly	n=2	-1	1	-1
	poly	n=3	-1	1	-1
	gaussian	σ=0.5	-1	1	-1
	gaussian	σ =1.5	-1	1	-1
ab-g fault at 30%,α=165°,R_f =50 ohm	poly	n=2	1	1	-1
	poly	n=3	1	1	-1
	gaussian	σ=0.5	1	1	-1
	gaussian	σ =1.5	1	1	-1
'bc' fault at 45%,α=170°,R_f =100 ohm	poly	n=2	-1	1	1
	poly	n=3	-1	1	1
	gaussian	σ=0.5	-1	1	1
	gaussian	σ =1.5	-1	1	1
'abc' fault at 65%,α=160°,R_f =200 ohm	poly	n=2	1	1	-1
	poly	n=3	1	1	1
	gaussian	σ=0.5	1	1	1
	gaussian	σ =1.5	1	1	1
'abc-g' fault at 75%,α=165°,R_f =150 ohm with source changed	poly	n=2	1	1	1
	poly	n=3	1	1	1
	gaussian	σ=0.5	-1	1	1
	gaussian	σ =1.5	1	1	1

TABLE II
CLASSIFICATION RATES OF SVM-1 FOR FAULT CLASSIFICATION WITH 200 DATA SETS

Fault	Kernel	Parameter value	Classification rates (%)	No. of support vectors
L-G	poly	n=2	96.52	15
	poly	n=3	97.23	12
	gaussian	σ=0.5	95.23	13
	gaussian	σ =1.5	96.85	11
LL-G	poly	n=2	96.27	9
	poly	n=3	97.36	7
	gaussian	σ=0.5	97.51	7
	gaussian	σ =0.5	97.84	7
LL	poly	n=2	96.84	11
	poly	n=3	97.29	9
	gaussian	σ=0.5	95.99	9
	gaussian	σ =1.5	96.87	6
LLL	poly	n=2	96.28	14
	poly	n=3	97.56	12
	gaussian	σ=0.5	95.68	11
	gaussian	σ =1.5	96.87	10
LLL-G	poly	n=2	97.25	12
	poly	n=3	97.68	10
	gaussian	σ=0.5	96.78	8
	gaussian	σ =1.5	97.65	5

kernel theory. Mercer's theorem states that any symmetric positive–definite matrix can be regarded as a kernel matrix.

The polynomial learning machines of degree "n" have the inner product kernel

$$K(x,z) = (x^T z + 1)^n \tag{10}$$

and radial basis function machines have the inner product kernel

$$K(x,z) = \exp\left\{-\frac{|x-z|^2}{2\sigma^2}\right\} \tag{11}$$

where the "σ" is the width of the Gaussian function.

IV. SVMS TRAINING AND TESTING

A. SVM for Fault Classification

The half-cycle fault current signal samples after the fault inception are taken as input to the SVM. The corresponding output is either a fault or no-fault condition. Ten samples (half cycle at 1.0-kHz sampling frequency) of fault current from the fault inception are retrieved at the relaying end are normalized along with the firing angle of TCSC and are used as input (11 inputs) space which is termed as "x." "y" is the corresponding output which results in "1" for fault and "-1" for no fault. The optimal marginal classifier is designed with a polynomial kernel with a different order and Gaussian kernel with a different parameter value. Both results are compared as depicted in Table I. The SVM-1 is trained with 500 data sets and tested with 200 data sets, each set comprised of 11 data points (10 for half cycle current signal and 1 for the firing angle of TCSC) for "x" as input and (1,-1) for "y" as corresponding output.

Faults on the line are simulated with various operating conditions including different incident angles, fault resistance (10 Ω–200 Ω), source capacities, and various locations with different firing angles for 11 types of shunt faults. When the parameter values of the polynomial kernel and Gaussian kernel are changed, the numbers of support vectors on the optimized marginal plane vary accordingly as seen from the result depicted in Table II. Here "n" stands for the order of the polynomial and "σ" stands for the width of the Gaussian function. The bound on the Lagrangian multipliers "C" is selected as 10 after testing the SVM for other values of "C." The conditioning parameter for QP method lambda is chosen as $1.0 * \mathrm{e} - 7$.

Table I shows the results for fault classification for various operating conditions. As seen from the table, for the "$b-g$" fault at 30%, $\alpha = 155°$, $R_f = 20\,\mathrm{ohm}$, the "b" ph output is "1" but the output for "a" and "c" phases is "-1" for both polynomial and Gaussian kernels, which depicts that the fault occurs only on the "b" phase. Also, for the "abc" fault at 65%, $\alpha = 160°$, $R_f = 200\,\mathrm{ohm}$, the output for all of the phases is "1." As seen, the misclassification occurs for the above operating condition with the polynomial kernel with "n"= 2 resulting in the output of "c" phase as "-1" instead of "1." Table II depicts the classification rates at different faults and corresponding support vectors with the polynomial and Gaussian kernel of different parameter values. The classification rate is 95.23% (minimum) at the L–G fault with a Gaussian kernel with $\sigma = 0.5$ and the support vectors are 13. Similarly, the classification rate is 97.84% (maximum) fir LL-G fault with a Gaussian kernel with $\sigma = 0.5$ which results seven support vectors on the hyperplane.

B. SVM for Ground Detection

The ground detection is done separately by training another SVM. The peak value of the zero-sequence component of the fault current signal for a half cycle is found out for the fundamental, third, and fifth harmonic component. The peak value of

TABLE III
TESTING OF SVM-2 FOR GROUND DETECTION

Fault	Kernel	Parameter value	Classification
a-g fault at 10%,α=160°,R_f =20 ohm	poly	n=1	1
	poly	n=2	1
	gaussian	σ =0.5	1
	gaussian	σ =1.0	1
bc fault at 30%,α=165°,R_f =50 ohm	poly	n=1	-1
	poly	n=2	-1
	gaussian	σ =0.5	-1
	gaussian	σ =1.0	-1
bc-g fault at 55%,α=175°,R_f =100 ohm	poly	n=1	1
	poly	n=2	1
	gaussian	σ =0.5	1
	gaussian	σ =1.0	1
abc fault at 65%,α=160°,R_f =150 ohm	poly	n=1	-1
	poly	n=2	-1
	gaussian	σ =0.5	-1
	gaussian	σ =1.0	-1
ac fault at 45%,α=155°,R_f =200 ohm	poly	n=1	-1
	poly	n=2	1
	gaussian	σ =0.5	-1
	gaussian	σ =1.0	-1
abc-g fault at 30%,α=165°,R_f =50 ohm	poly	n=1	1
	poly	n=2	1
	gaussian	σ =0.5	1
	gaussian	σ =1.0	1
bc-g fault at 85%,α=165°,R_f =100 ohm	poly	n=1	1
	poly	n=2	1
	gaussian	σ =0.5	1
	gaussian	σ =1.0	1
ab fault at 65%,α=160°,R_f =150 ohm	poly	n=1	-1
	poly	n=2	-1
	gaussian	σ =0.5	-1
	gaussian	σ =1.0	-1
abc-g fault at 85%,α=160°,R_f =150 ohm with source changed	poly	n=1	-1
	poly	n=2	1
	gaussian	σ =0.5	1
	gaussian	σ =1.0	1

TABLE IV
TESTING OF SVM-3 FOR SECTION IDENTIFICATION

Fault	Kernel	Parameter value	Classification
ab fault at 10%,α=160°,R_f =20 ohm	poly	n=1	-1
	poly	n=2	-1
	gaussian	σ =0.5	-1
	gaussian	σ =1.0	-1
ac-g fault at 30%,α=165°,R_f =50 ohm	poly	n=1	-1
	poly	n=2	-1
	gaussian	σ =0.5	-1
	gaussian	σ =1.0	-1
bc-g fault at 55%,α=170°,R_f =100 ohm	poly	n=1	1
	poly	n=2	1
	gaussian	σ =0.5	1
	gaussian	σ =1.0	1
abc-g fault at 65%,α=170°,R_f =150 ohm	poly	n=1	1
	poly	n=2	1
	gaussian	σ =0.5	1
	gaussian	σ =1.0	1
ac fault at 45%,α=165°,R_f =100 ohm	poly	n=1	-1
	poly	n=2	-1
	gaussian	σ =0.5	-1
	gaussian	σ =1.0	-1
abc-g fault at 30%,α=175°,R_f =20 ohm	poly	n=1	1
	poly	n=2	-1
	gaussian	σ =0.5	-1
	gaussian	σ =1.0	-1
bc-g fault at 75%,α=165°,R_f =100 ohm with source changed	poly	n=1	1
	poly	n=2	1
	gaussian	σ =0.5	1
	gaussian	σ =1.0	1
ab fault at 15%,α=160°,R_f =20 ohm with source changed	poly	n=1	-1
	poly	n=2	-1
	gaussian	σ =0.5	1
	gaussian	σ =1.0	-1
abc fault at 65%,α=155°,R_f =200 ohm with source changed	poly	n=1	1
	poly	n=2	-1
	gaussian	σ =0.5	1
	gaussian	σ =1.0	1

zero-sequence components and firing angle of TCSC are used as the input-"x" (4 inputs) to the SVM-2 and the corresponding output (y) is "1" for the fault involving ground and "-1" for the fault without involving ground. As the zero-sequence components for these three harmonic components are pronounced in case of a fault involving the ground compared to a fault without involving ground, the SVM-2 is trained to design an optimized classifier for ground detection.

The order of the polynomial is "n" and the width of the Gaussian function is "σ." The Lagrangian parameter is selected after testing the SVM with other values, but $C = 5.0$ provides the best result compared to other values. Thus, the bound on the lagrangian multipliers "C" is selected 5.0 and the conditioning parameter for the QP method lambda is chosen as $1.0 * \mathrm{e} - 7$. The SVM is trained with 500 data sets and tested for 200 data sets. The average classification rate for ground detection for 200 test cases is found to be 98.05% for all types of faults with different operating conditions. It is found from Table III that for an "a-g" fault at 10%, $\alpha = 160°$, $R_f = 20\,\mathrm{ohm}$, the output is "1" which shows that the fault involves ground. But the "bc" fault at 30%, $\alpha = 165°$, $R_f = 50\,\mathrm{ohm}$, the output is "-1" which clearly shows that fault without involving ground. Also, misclassification is observed for the ac fault at 45%, $\alpha = 155°$, $R_f = 200\,\mathrm{ohm}$ with the polynomial kernel for $n = 2$, which produces output "1" instead of "-1." Also, a similar case occurs for the abc-g fault at 85% $\alpha = 160°$, $R_f = 150\,\mathrm{ohm}$ with a polynomial kernel for $n = 1$.

C. SVM for Section Identification

Section identification for the transmission line with TCSC is accomplished by training the SVM-3 to build up an optimized classifier. The half-cycle data (ten samples) after the fault inception and firing angle of TCSC are used as input-"x" (11 inputs) to the SVM and the output-"y" is the output. The output "y" is "1" or "-1" for faults including TCSC and without TCSC, respectively. For any fault beyond 50% of the line, the output of the SVM should be "1," otherwise "-1." The SVM is trained with the bound on the Lagrangian multipliers with "C" selected as 20 and the conditioning parameter for QP method lambda chosen as $1.0 * \mathrm{e} - 7$. The Lagrangian parameter "C"' is selected after testing the SVM with other values. The SVM is trained with 500 data sets and tested for 200 data sets. The average classification rate for section identification for 200 test

cases is found to be 95.09% for all types of faults with different operating conditions.

Table IV depicts the results for section identification for TCSC on the transmission line. For the "ac-g" fault at 30%, $\alpha = 165°$, $R_f = 50$ ohm, the output of SVM is "−1" which shows that the fault occurred before TCSC on the line. But for the "bc-g" fault at 55%, $\alpha = 170°$, $R_f = 100$ ohm, the output of SVM is "1," which clearly depicts that the fault occurred after the TCSC on the line. Also, misclassification is observed for the "abc-g" fault at 30%, $\alpha = 175°$, $R_f = 20$ ohm with a polynomial kernel with $\mathrm{n} = 1$ and for the "ab" fault at 15%, $\alpha = 160°$, $R_f = 20$ ohm with source changed with a Gaussian kernel with $\sigma = 0.5$. Also, a similar result occurs for the "abc" fault at 65% $\alpha = 155°$, $R_f = 200$ ohm with a source changed for the polynomial kernel with $n = 2$.

V. Conclusion

A new approach for the protection of a flexible ac transmission Line with TCSC using the SVM is presented in this paper. Half-cycle postfault current samples and firing angles are used as input to the SVMs and the output is the corresponding classification. SVM-1 is used for fault classification, SVM-2 is used for ground detection, and SVM-3 is used for section identification for the TCSC on the line, respectively. It is found that SVMs are trained to result in most optimized classifier and with less numbers of training samples compared to the neural network and neuro-fuzzy systems. Also, the error found is less than 5%, taking all SVMs into consideration. Hence, the proposed method is very accurate and robust for the protection of transmission line including TCSC.

References

[1] A. A. Girgis, A. A. Sallam, and A. K. El-din, "An adaptive protection scheme foe advanced series compensated (ASC) transmission line," *IEEE Trans. Power Del.*, vol. 13, no. 1, pp. 414–420, Apr. 1998.

[2] S. G. Helbing and G. G. Karady, "Investigations of an advanced form of series compensation," *IEEE Trans. Power Del.*, vol. 9, no. 2, pp. 939–946, Apr. 1994.

[3] E. V. Larsen, K. Clark, S. A. Miske, and J. Urbanek, "Characteristics and rating considerations of thyristor controlled series compensation," *IEEE Trans. Power Del.*, vol. 9, no. 2, pp. 992–1000, Apr. 1994.

[4] Y. H. Song, Q. Y. Xuan, and A. T. Johns, "Protection of scheme for EHV transmission systems with thyristor controlled series compensation using radial basis function neural networks," *Elect. Mach. Power Syst.*, vol. 25, pp. 553–565, 1997.

[5] Y. H. Song, A. T. Johns, and Q. Y. Xuan, "Artificial neural network based protection scheme for controllable series-compensated EHV transmission lines," *Proc. Inst. Elect. Eng., Gen. Transm. Distrib.*, vol. 143, no. 6, pp. 535–540, 1996.

[6] M. Noroozian, L. Angquist, M. Ghandhari, and G. Anderson, "Improving power system dynamics by series connected FACTS devices," *IEEE Trans. Power Del.*, vol. 12, no. 4, pp. 1635–1641, Oct. 1997.

[7] P. K. Dash, A. K. Pradhan, G. Panda, and A. C. Liew, "Adaptive relay setting for Flexible AC Transmission Systems (FACTS)," *IEEE Trans. Power Del.*, vol. 15, no. 1, pp. 38–43, Jan. 2000.

[8] C. J. C. Burges, "A tutorial on support vector machines for pattern recognition," *Data Mining Knowl. Discov.*, vol. 2, no. 2, pp. l21–167, 1998.

[9] ——, "Geometry and invariance in kernel based methods," in *Advances in Kernel Methods-Support Vector Learning* B. Schoelkopf, C. J. C. Burges, and A. J. Smola, Eds. Cambridge, MA: MIT Press, 1999, pp. 89–116.

[10] O. Chapelle and V. N. Vapnik, "Model selection for support vector machines," in *Advances in Neural Information Processing Systems*, S. Solla, T. K. Leen, and K.-R. Muller, Eds. Cambridge, MA: MIT Press, 2000, vol. 12, pp. 230–236.

[11] C. Bregler, "Learning and recognizing human dynamics in video sequences," in *R. Nevatia*, G. Medioni, Ed. Silver Spring, MD: IEEE Comput. Soc. Press, 1997, pp. 568–574.

[12] O. Chapelle, V. N. Vapnik, O. Bousquet, and S. Mukherjee, "Choosing multiple parameters for support vector machines," *Mach. Learn.*, vol. 46, no. 1–3, pp. 131–159, 2002.

[13] R. Collobert and S. Bangio, "SVMTorch: A support vector machine for large-scale regression and classifcation problems," *J. Mach. Learn. Res.*, vol. 1, pp. 143–160, 2001.

[14] N. Cristianini and J. Shawe-Taylor, *An Introduction to Support Vector Machines and Other Kernel-Based Learning Methods*. Cambridge, U.K.: Cambridge Univ. Press, 2000.

[15] Y. Yajima, H. Ohi, and M. Mori, "Extracting feature subspace for kernel based support vector machines" Dept. Ind. Eng. Manage., Tokyo Inst. Technol., Tech. Rep. 2001-5, 2001.

[16] O. L. Mangasarian and D. R. Musicant, "Successive overrelaxation for support vector machines," *IEEE Trans. Neural Netw.*, vol. 10, no. 5, pp. 1032–1037, Sep. 1999.

P. K. Dash (SM'90) received the D.Sc., Ph.D., M.E., and B.E. degrees in electrical engineering and the Postdoctoral degree from the University of Calgary, Calgary, AB, Canada.

Currently, he is Director of the College of Engineering, Bhubaneswar, India. He was a Professor in the Faculty of Engineering, Multimedia University, and Cyberjaya, Malaysia. He also was a Professor of Electrical Engineering and Chairman of the Center for Intelligent Systems, National Institute of Technology, Rourkela, India, for more than 25 years. His research interests are power quality, FACTS, soft computing, deregulation and energy markets, signal processing, and data mining and control. He had several visiting appointments in Canada, the U.S., Switzerland, and Singapore. He has published many international journal papers and international conferences.

Prof. Dash is a Fellow of the Indian National Academy of Engineering and a Fellow of the Institution of Engineers, India.

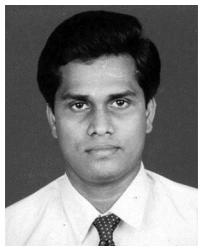

S. R. Samantaray is currently pursuing the Ph.D. degree in the area of intelligent protection to power systems with the National Institute of Technology (NIST), Rourkela, India.

He has worked with the National Institute of Technology (NIT) Rourkela, Rourkela. He has worked with the TATA Refractories Ltd. in the area of power system and industrial automation and instrumentation. His research interests include flexible ac transmission systems (FACTS), power quality, digital signal processing, and computational intelligence.

Ganapati Panda (SM'97) received the Ph.D. degree in digital signal processing from the Indian Institute of Technology, Kharagpur, India, in 1982, and the Postdoctoral degree from the University of Edinburgh, Edinburgh, U.K., in 1984–1986.

Currently, he is a Professor in the Department of Electronics and Communications Engineering with the National Institute of Technology, Rourkela, India. He has published many papers in referred research journals and conferences. He carries out research work in the field of digital signal processing (DSP), soft computing, and digital communication.

Dr. Panda is a Fellow of INAE and the National Academy of Science, India.